

**LA-7823-M**

Manual  
(ISPO-66)

## **Description and Operation Manual for the Active Well Coincidence Counter**

University of California



**LOS ALAMOS SCIENTIFIC LABORATORY**

Post Office Box 1663 Los Alamos, New Mexico 87545

USA

IAEA

PROGRAM FOR  
TECHNICAL ASSISTANCE  
TO IAEA SAFEGUARDS

Department of Energy  
Safeguards & Security

This report was not edited by the Technical Information staff.

This work was supported by the US Department of Energy, Office of Safeguards and Security, and by the Program for Technical Assistance to IAEA Safeguards.

This report was prepared as an account of work sponsored by an Agency of the United States Government. Neither the United States nor the United States Department of Energy, nor any of their employees, nor any of their contractors, sub-contractors, or their employees, makes any warranty, express or implied, or assumes any legal liability or responsibility for the accuracy, completeness, or usefulness of any information, apparatus, product, or process disclosed, or represents that its use would not infringe privately owned rights. Further, neither the subject matter nor the content of this report reflects any policy, expressed or implied, by the United States Government.

**LA-7823-M**  
**Manual**  
**(ISPO-66)**

**Special Distribution**  
**Issued: May 1979**

# **Description and Operation Manual for the Active Well Coincidence Counter**

**Howard O. Menlove**



## CONTENTS

FIGURES . . . . .	
TABLES . . . . .	
ABSTRACT . . . . .	1
I. INTRODUCTION . . . . .	1
II. SYSTEM DESCRIPTION . . . . .	3
A. Detector Body . . . . .	3
B. Neutron Sources . . . . .	4
C. End Plugs for the Neutron Sources . . . . .	4
D. Neutron Detector Tubes . . . . .	7
E. Electronics . . . . .	9
F. Detector Cart and Portability . . . . .	9
III. OPERATION OF ASSAY SYSTEM . . . . .	10
A. Sample Categories . . . . .	10
B. Normal Setup . . . . .	13
C. Measurement Steps . . . . .	14
D. Calibration . . . . .	15
IV. PERFORMANCE CHARACTERISTICS . . . . .	16
A. Introduction . . . . .	16
B. Sample Position Effects . . . . .	17
C. Neutron Interrogation Penetrability . . . . .	19
D. System Stability . . . . .	22
ACKNOWLEDGEMENTS . . . . .	22
APPENDICES	
A. Calculation of Performance Characteristics . . . . .	23
B. Thermal-Mode Operation . . . . .	25
C. Error Calculation and Gate Length Selection . . . . .	27
D. Passive-Mode Operation . . . . .	29
REFERENCES . . . . .	30



## FIGURES

1. Schematic diagram of Active Well Coincidence Counter (AWCC) showing normal configuration of end plugs and AmLi neutron sources . . . . . 4
2. Photograph of AmLi neutron source inside its tungsten container (or pipe) . . . . . 5
3. Schematic diagram of tungsten holder for the AmLi neutron sources . . . . . 5
4. Schematic diagram of end plugs and sample cavity for "normal" measurement configuration . . . . . 6
5. Schematic diagram of end plugs and sample cavity for maximum sample volume . . . . . 7
6. Photograph of  $^3\text{He}$  detector ring partially removed from the CH<sub>2</sub> body . . . . . 8
7. Top view of HV distribution box with cover removed to show wiring hook-ups to the  $^3\text{He}$  tubes for the 6 lines of electronics . . . . . 9
8. Back view of AWCC and preamp box with the electronic support tray down in position for shipment . . . . . 10
9. Electronic package including the shift register unit which is directly interfaced into the HP-97 calculator . . . . . 11
10. Photograph of complete AWCC system including detector, cart, and electronics for automated data collection and analyses . . . . . 12
11. High-enrichment (93%  $^{235}\text{U}$ ) uranium metal discs (or buttons) which are clad with nickel to prevent contamination . . . . . 12
12. Top view of AWCC showing sample chamber and typical can containing U<sub>3</sub>O<sub>8</sub> . . . . . 13
13. Schematic diagram of AWCC showing side operation to accommodate long samples such as fuel rods and trays . . . . . 14
14. Coincidence response as sample fill height for the AWCC in normal configuration (see Fig. 4) using single source (bottom curves) and double source (top curve) . . . . . 18

15.	Vertical and radial coincidence response vs sample position for a small disc sample. The AWCC is in its normal configuration as shown in Fig. 4 . . . . .	20
16.	Coincidence response vs sample fill height for the AWCC using single source (bottom curves) and double source (top curve). In this case the cavity is opened to a 30 cm vertical height . . . . .	20
17.	Coincidence response vs uranium mass for HEU metal buttons in the AWCC with (top curve) and without (bottom curve) the Ni liner . . . . .	21
18.	Calculated relative precision as a function of neutron interrogation source strength for the HLNCC and the AWCC with 20-cm-high sample cavities . . . . .	25
19.	Coincidence rate vs $^{235}\text{U}$ mass for low enrichment $\text{U}_3\text{O}_8$ samples and thermal-neutron interrogation mode . . . . .	27
20.	Normalized coincidence rate vs gate width for the HLNCC and the AWCC . . . . .	29
21.	Relative assay error vs gate width with the error normalized to unity at its minimum value ( $\sim 64 \mu\text{s}$ ) . . . . .	29

## TABLES

I.	$^{241}\text{AmO}_2$ -Li NEUTRON SOURCE CHARACTERISTICS . . . . .	5
II.	END PLUG CONFIGURATIONS . . . . .	6
III.	PERFORMANCE CHARACTERISTICS OF AWCC . . . . .	17
IV.	GEOMETRIC EFFECT OF SAMPLE FILL-HEIGHT ON COINCIDENCE RESPONSE FOR 20-cm HIGH CAVITY . . . . .	19



# DESCRIPTION AND OPERATION MANUAL FOR THE ACTIVE WELL COINCIDENCE COUNTER

by

Howard O. Menlove

## ABSTRACT

An Active Well Coincidence Counter (AWCC) has been developed to assay uranium fuel material in field inspection applications. The operation of the AWCC is based on active neutron interrogation using a small AmLi neutron source and counting the induced fission neutrons with high-efficiency  $^3\text{He}$  detectors operated in the coincidence mode. In comparison with the conventional fast random driver assay system, the AWCC is more portable, lightweight, stable and less subject to gamma-ray backgrounds.

The unit is useful for the measurement of bulk  $\text{UO}_2$  samples, high-enrichment uranium metals, LWR fuel pellets, and  $^{233}\text{U}$ -Th fuel materials, which have very high gamma-ray backgrounds. By removing the AmLi source, the unit can measure  $^{238}\text{U}$  and plutonium in the passive neutron coincidence mode.

This manual describes the system components, setup, calibration, and operation of the AWCC, which has been developed for field inspection applications by IAEA inspectors.

---

## I. INTRODUCTION

The passive neutron well coincidence counter has proven to be one of the most useful NDA instrument for plutonium assay. IAEA inspectors have found the portable high-level neutron coincidence counter (HLNCC) unit<sup>1</sup> particularly useful for field applications. However, the instrument has not been applicable to the assay of  $^{235}\text{U}$  or  $^{233}\text{U}$  because of their extremely low spontaneous fission yields. To make this type instrument applicable to the two uranium isotopes, we have used a combination of a small

AmLi neutron interrogation source and a  $^3\text{He}$  thermal-neutron well coincidence counter. This Active Well Coincidence Counter (AWCC)<sup>2</sup> can be used for uranium samples, including high gamma-ray background materials such as  $^{233}\text{U}$ -Th fuels of special interest for alternative fuel cycle concepts.

This type instrumentation was first investigated by J. Foley<sup>3</sup> in 1971; however, at that time, the electronics for coincidence counting were not advanced enough to handle the high accidental background rates from the  $(\alpha, n)$  neutron source. Also, no special shielding techniques were used to reduce the neutron background from the interrogation source.

In comparison with the conventional fast random driver (RD),<sup>4</sup> the neutron well coincidence counter is more portable, lightweight, stable, and less subject to effects of matrix materials and gamma-ray backgrounds. This last feature makes it applicable to  $^{233}\text{U}$ -Th fuel cycle materials which generally have very high gamma-ray backgrounds from the decay of  $^{232}\text{U}$ .

In the past, when an interrogation source was used with the thermal-neutron well coincidence counter, the 30- to 100- $\mu\text{s}$  gate lengths results in a pile-up of accidental counts from the random interrogation source (AmLi). To alleviate this problem, we are positioning the AmLi source inside  $\text{CH}_2$  shielding to take advantage of the greater transmission of the induced prompt fission neutrons (1- to 2-MeV average energy) compared with the AmLi neutrons ( $\sim 400$ -keV average energy). With this technique, the induced signal-to-interrogation neutron background ratio can be improved by more than an order of magnitude.

The AWCC can also be used for the passive assay of plutonium by removing the small ( $\sim 5 \times 10^4$  n/s) AmLi neutron sources. Because the efficiency of the AWCC is about three times higher than the HLNCC, the coincidence counting rate will be about an order of magnitude higher for the AWCC.

The AWCC has been designed to take advantage of the portable electronics package<sup>5</sup> that was developed for the HLNCC. To keep this initial model as simple as possible and to take direct advantage of the previously developed electronics package, no neutron



flux monitor has been incorporated into the present AWCC. Flux monitors are often used with active neutron assay units to make corrections for neutron self-shielding or for neutron moderation in homogeneous matrix materials. Operational experience with the present model will be used to evaluate the need for a flux monitor in more advanced models.

## II. SYSTEM DESCRIPTION

### A. Detector Body

Figure 1 is a schematic of the AWCC which has a design optimized for counting the induced-fission reactions and discriminating against the lower energy AmLi background neutrons. The sample cavity wall is lined with a 2.54-cm-thick nickel reflector to give a more penetrating neutron interrogation. The CH<sub>2</sub> moderator and cadmium sleeves are designed to give maximum efficiency for counting the induced-fission spectrum neutrons and at the same time have a low efficiency for counting the ( $\alpha$ ,n) neutrons from the AmLi interrogation source. The optimum CH<sub>2</sub> moderator thickness between the sample and the <sup>3</sup>He tube is ~5 cm for fission neutrons and ~2 cm for AmLi neutrons. Thus, the thick CH<sub>2</sub> in the end plugs and wall of the well detector forms a neutron shield to reduce the AmLi counting efficiency. If the CH<sub>2</sub> shielding material is removed from the end plug, the background totals rate from the AmLi source increases by a factor of ~5 and the coincidence background rate by a factor of ~25. This selective shielding of the interrogation source is the primary factor making it possible to use the <sup>3</sup>He thermal-neutron detectors with their long coincidence gate length requirements.

The nickel reflector on the wall of the interrogation cavity gives a more penetrating neutron irradiation and a slightly better statistical precision. With the nickel in place, the maximum sample diameter is 17 cm. For larger samples, the nickel can be removed giving a sample cavity diameter of 22 cm.

A cadmium sleeve is placed on the outside of the detector to reduce the background rate from low energy neutrons in the room. There is also a sleeve of Cd in the detector well to remove

thermal neutrons from the interrogation flux and to improve the shielding between the  $^3\text{He}$  detectors and the AmLi source.

### B. Neutron Sources

The present AWCC uses two AmLi neutron sources purchased from Monsanto Research Corporation, Dayton, Ohio. Table 1 lists the characteristics of the sources and Fig. 2 is a photograph of one of the sources. Figure 3 is a schematic diagram of the tungsten shield, fabricated at LASL, that is placed around the AmLi source to reduce the gamma-ray dose. The source gives a dose of 0.4 rem/h in air at a distance of 30 cm and less than 0.1 rem/h at the surface of the assay system.

The AmLi sources have a long half-life (432 yr) so the original source will last for the life of the assay system.

The optimum source strength for the present AWCC is  $5 \times 10^4$  n/s for each source. Details leading to this source yield selection are given in Appendix A.

To obtain a more uniform spatial interrogation, two neutron sources of similar yield are used. One is in the lid and one is in the bottom plug as shown in Fig. 1. The use of two sources results in a rather uniform vertical response as shown in Section IV-B.

### C. End Plugs for the Neutron Sources

The lid and bottom plug serve as the neutron shields for the AmLi interrogation sources and also as reflectors to increase counting efficiency by reducing neutron end losses. They are made

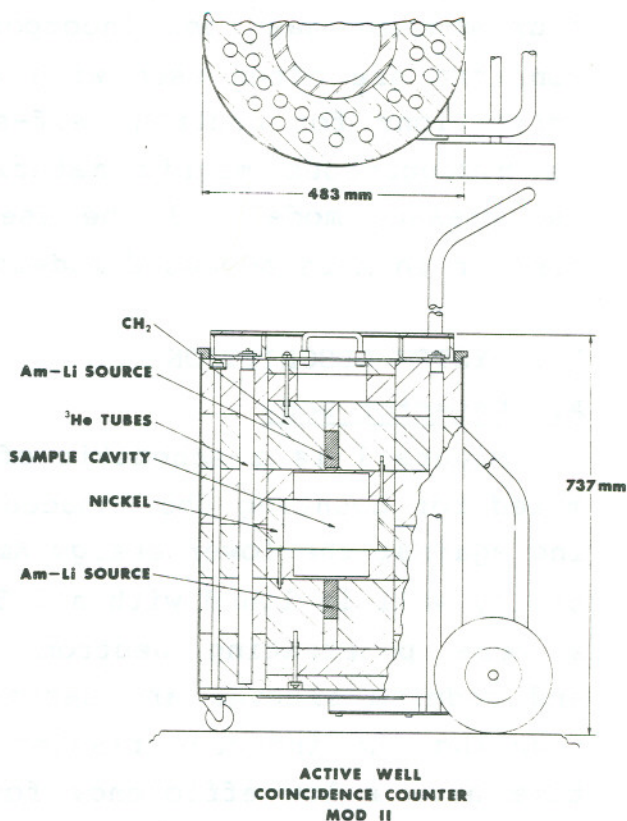


Fig. 1.  
Schematic diagram of Active Well Coincidence Counter (AWCC) showing normal configuration of end plugs and AmLi neutron sources.



TABLE I  
 $^{241}\text{AmO}_2\text{-Li}$  NEUTRON SOURCE CHARACTERISTICS

Source Number	Am't of $^{241}\text{Am}$	Li	Emission Rate
MRC-AmLi-79	0.68 Ci or 0.198 g	1.4 g	$4.8 \times 10^4 \text{ n/s}$
MRC-AmLi-80	0.66 Ci or 0.191 g	1.4 g	$4.6 \times 10^4 \text{ n/s}$

Technical Information

Chemical Form:	$\text{AmO}_2$
Isotope:	Am-241
Source Container Description:	MRC Model 24132; Stainless Steel 20 mm O.D. x 50 mm O.L.
Shipping Container:	10 gal drum, 6M-1023 USDOT Spec. 6m, Type B



Fig. 2.  
 Photograph of AmLi neutron source inside its tungsten container (or pipe).

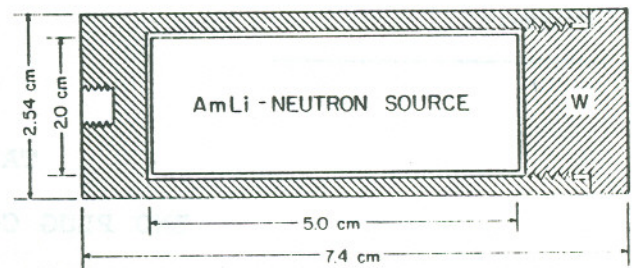


Fig. 3.  
 Schematic diagram of tungsten holder for the AmLi neutron sources.

of  $\text{CH}_2$  with Cd plates (0.81 mm thick) on the ends adjacent to the sample to prevent thermal neutrons from entering the interrogation cavity.

Figure 4 shows a diagram of the end plugs and interrogation cavity. The plugs have removable  $\text{CH}_2$  discs which serve as spacers and can be removed to effectively increase the height of the sample chamber.. By removing the 2.54-cm-thick discs on the

top and bottom plugs, the cavity will accommodate a sample that is 25 cm tall. Larger sizes can be accommodated by removing additional discs as listed in Table II. The purpose of the CH<sub>2</sub> spacers is to give a higher interrogation flux for small samples (<20 cm high) by positioning the AmLi sources closer to the sample. The discs are removable to accommodate larger samples when necessary. The spacer discs should always be removed the same in the top and bottom plugs to maintain the spatial interrogation symmetry in the sample chamber.

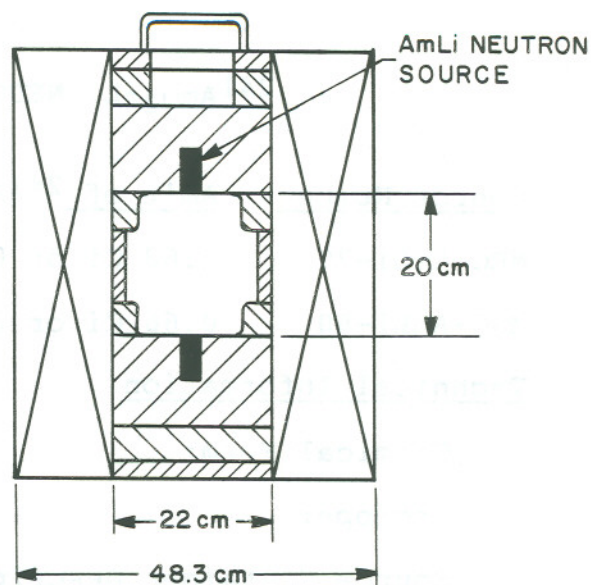


Fig. 4.  
Schematic diagram of end plugs and sample cavity for "normal" measurement configuration.

TABLE II  
END PLUG CONFIGURATIONS

<u>Plug Configuration</u>	<u>Cavity Height</u>	<u>Passive Counting Efficiency<sup>a</sup></u>	<u>Relative Assay Time<sup>b</sup></u>
Full discs	20 cm	26%	1.00
Small disc removed	25 cm	28%	1.44
Both discs removed	35 cm	31%	3.03

(a) Passive efficiency corresponds to absolute totals efficiency for a spontaneous fission source (<sup>252</sup>Cf) placed in the center of the sample chamber.

(b) Corresponds to relative measurement time to reach the same precision for the same sample.



The 4-cm-thick  $\text{CH}_2$  ring on the sample cavity side of both end plugs has the function of shielding the AmLi sources from the  $^3\text{He}$  detectors. This ring can be removed if necessary because of sample size.

Because changing the spacer configuration changes the interrogation flux and counting efficiency, the calibration must always be done with the same configuration as the actual assay.

Table II lists the efficiency for counting the fission neutrons from the center of the well and the relative assay time for the different end plug configurations. As expected, the measurement precision is best when the sample cavity is the smallest. Somewhat unexpected, the passive counting efficiency increases for the larger cavity configurations. This is caused by the larger end plugs shielding the ends of the  $^3\text{He}$  tubes from the fission neutron source.

Figure 5 gives a schematic diagram of the AWCC in the configuration for maximum sample volume. Any deviations from the normal configuration as shown in Fig. 4 should be carefully documented at the time of calibration and subsequent assay.

#### D. Neutron Detector Tubes

The unit uses 42- $^3\text{He}$  gas tubes (Reuter-Stokes model RS-P4-0820-107-W) that are 2.54 cm diameter and 50.8 cm long (active length). The  $^3\text{He}$  gas has 5%  $\text{CO}_2$  added to improve gamma-ray insensitivity as compared to the normal additives. Experimental tests<sup>6</sup> have shown that this gas mixture is better for gamma-ray insensitivity than the normal mixture that is used by Reuter-Stokes to get the best resolution. Good energy resolution is not important for the present application. The detectors are matched to operate at the same high voltage ( $\sim 1500$  V) with a resolution of approximately 9%.

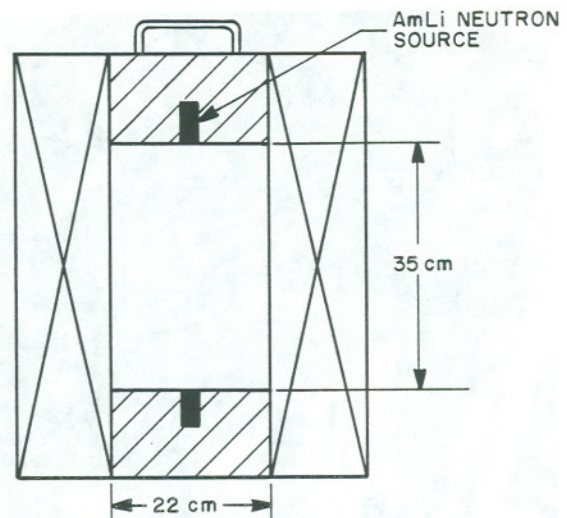


Fig. 5.  
Schematic diagram of end plugs and sample cavity for maximum sample volume.





Fig. 6.

Photograph of  $^3\text{He}$  detector ring partially removed from the  $\text{CH}_2$  body.

Figure 6 shows the top of the AWCC with the detector bank raised about 10 cm to show the individual  $^3\text{He}$  tubes in the  $\text{CH}_2$  matrix. The top annulus shown in Fig. 7 is the high voltage distribution box which is used to connect the detector tubes with the high-voltage (HV) and signal leads. The detectors are wired to give 6 groups of 7 tubes each. The 6 separate lines of electronics fed into the preamplifier box attached to the back of the AWCC under the handle as shown in Fig. 8. For high counting rate applications, the main source of deadtime is the pulse pileup in the amplifier. Thus, the 6 amplifiers lines are used to reduce the rate on each individual line.



The HV junction box shown in Fig. 7 contains a desiccant to reduce the moisture content in the box to prevent HV breakdown. The lid of the junction box is sealed to the body with a rubber gasket.

#### E. Electronics

The electronics for the present unit are the same as that used for the HLNCC.<sup>5</sup> The preamp box shown in Fig. 8 contains the HV input for the  $^3\text{He}$  detectors and separate preamps for the 6 lines of electronics. This box stays attached to the AWCC during use and transit. The signal leads from the preamp box are connected to the main electronics package shown in Fig. 9. This unit contains the HV and low voltage power supplies, 6 amplifier discriminator lines, a microprocessor, and the shift register<sup>7</sup> coincidence logic.

The electronics unit is directly interfaced to the HP-97 programmable calculator shown in Fig. 9. A microprocessor in the unit reads out the run time, total counts, reals plus accidental counts, and accidental counts to the HP-97. The HP-97 is then used to reduce the data using the software package selected by the operator.

Details concerning the design, fabrication, and operation of the electronics system is published elsewhere.<sup>1,5,7</sup>

#### F. Detector Cart and Portability

A side view of the AWCC cart is shown in Fig. 10. This cart is a standard hand truck (Harper Model No. 5214) which has been modified to accommodate the detector and electronics package. The detector is attached to the cart and it stays attached for both

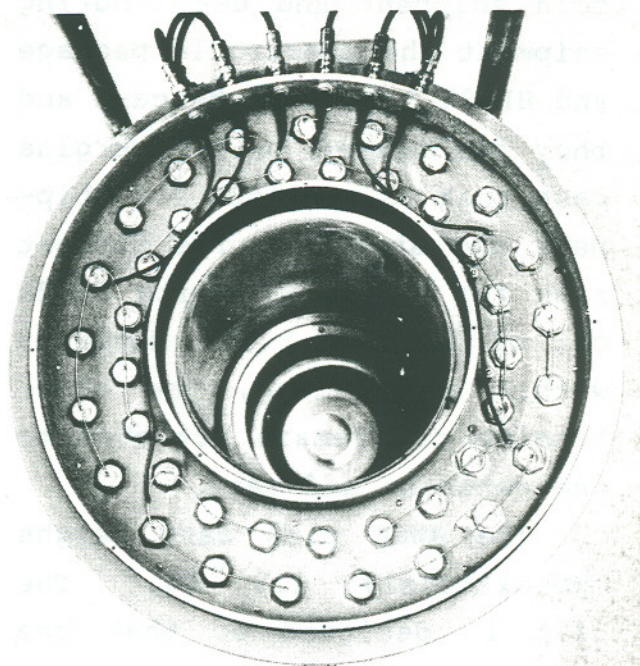


Fig. 7.  
Top view of HV distribution box with cover removed to show wiring hook-ups to the  $^3\text{He}$  tubes for the 6 lines of electronics.



both shipment and use. During shipment the electronic package and HP-97 lift off the cart and they are placed in a Fiberglas case that is provided for shipment and storage. The support rack for the electronics folds out of the way. For movement within a building, the electronics can remain attached to the detector and cart.

The AWCC plus cart weighs approximately 125 kg. The cart is designed so that one person can move the unit over minor obstacles such as small steps.

### III. OPERATION OF ASSAY SYSTEM

#### A. Sample Categories

The assay system can be applied to a wide variety of sample types. For the important case of  $\text{PuO}_2$  and plutonium metal, the AmLi sources are removed from the top and bottom end plugs, the unit then operates the same as the HLNCC but with substantially higher efficiency.

Active mode, neutron interrogation is used for  $^{235}\text{U}$  and  $^{233}\text{U}$  assay. These materials are typically found in the form of metal buttons, cans of  $\text{UO}_2$  powder and

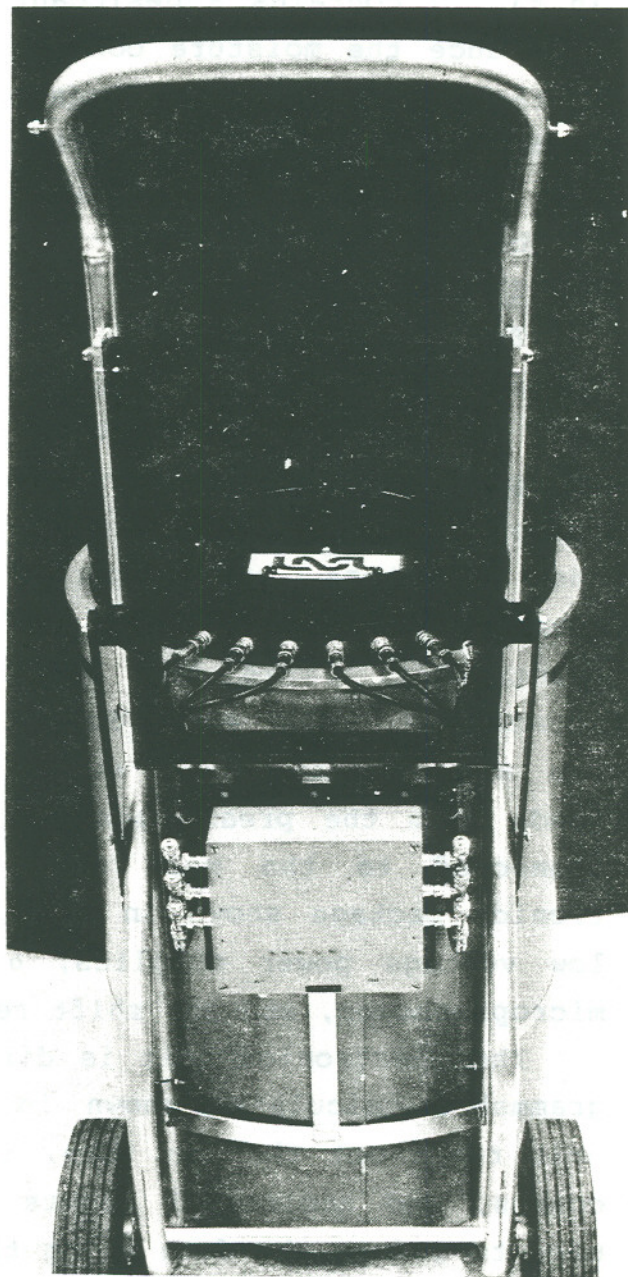


Fig. 8.

Back view of AWCC and preamp box with the electronic support tray down in position for shipment.





Fig. 9.

Electronic package including the shift register unit which is directly interfaced into the HP-97 calculator.

pellets, U-Al alloy scrap, and fuel rods. Examples of the HEU-buttons and  $UO_2$  powder are shown in Figs. 11 and 12, respectively.

For most cases the counter should be operated in the "normal" configuration as shown in Fig. 4. If the sample is too large to fit in the cavity, the spacer discs and/or Ni liner can be removed as needed.





Fig. 10.

Photograph of complete AWCC system including detector, cart, and electronics for automated data collection and analyses.



Fig. 11.

High-enrichment (93%  $^{235}\text{U}$ ) uranium metal discs (or buttons) which are clad with nickel to prevent contamination.

For those cases where a thermal-neutron mode of operation is desired (e.g., low enrichment  $\text{UO}_2$  or low content scrap), the inside Cd sleeve can be pulled out and the Cd caps can be removed from the end plugs. This operation requires a screw driver and normally takes about 10 minutes to complete.

For application to long samples such as fuel rods or plates which will not fit inside the closed cavity (i.e., lengths greater than 45 cm), the unit can be turned on its side and the end plugs removed as shown in Fig. 13. The electronic unit support arm must be closed and the electronics can be placed on a nearby table or the floor.



The two AmLi neutron sources should be removed from the end plugs and placed in the  $\text{CH}_2$  holder which is positioned in the center of the through hole as shown in Fig. 13. In this mode of operation, there is a sharp drop off in the interrogation efficiency as a function of axial position out from the center of the detector. Thus, to uniformly measure the material, the sample must be scanned along the axis. Alternatively, for limited sample lengths, a two position measurement technique<sup>1</sup> can be used.

#### B. Normal Setup

1. Remove AWCC unit from shipping container or storage location, and wheel to desired measurement location. If possible, select a location without high neutron backgrounds.

2. Open sample well and check that the end plugs are in the "normal" configuration.

Check that the Cd sleeves and Ni liner are in place.

3. Remove all storage parts from the sample cavity.

4. Lift up the support arm for the electronic package and hook it to the top of the cart.

5. Place the electronic unit on the support with the HP-97 on top of the electronic unit as shown in Fig. 9.



Fig. 12.  
Top view of AWCC showing sample chamber and typical can containing  $\text{U}_3\text{O}_8$ .



6. Connect the multiwire cord and the SHV cable between the back of the shift register electronics unit and the preamp box mounted on the cart. Also connect the ribbon on the HP-97 to the back of the electronics unit.

7. Confirm that all switches and dials are in the proper positions (see Ref. 1) before plugging in the ac line cord.

8. Turn on the power switch and the HV. The HV and discriminator should be set to the same values as when the calibration was performed. The normal settings for the HV is 1510 V, the discriminator level is 3.0 V, and the gate is 64  $\mu$ s.

9. Remove the end plugs (i.e., the AmLi sources) and measure the room background. This background rate should not be higher than a few hundred counts per second. The end plugs should be removed far enough from the detector that they do not significantly contribute to the rate.

10. With the end plugs back in the normal configuration, take a 100 s count and check that the net totals rate is statistically the same as when calibration took place. Also check that the net coincidence rate is statistically equal to zero.

11. If no problems have been encountered, the unit is ready to receive the desired software program in the HP-97. Instructions for a more complete check-out of the electronics system is given in reference 1.

### C. Measurement Steps

1. Before placing the first sample in well, take a 100 s background run to establish room plus source background levels.

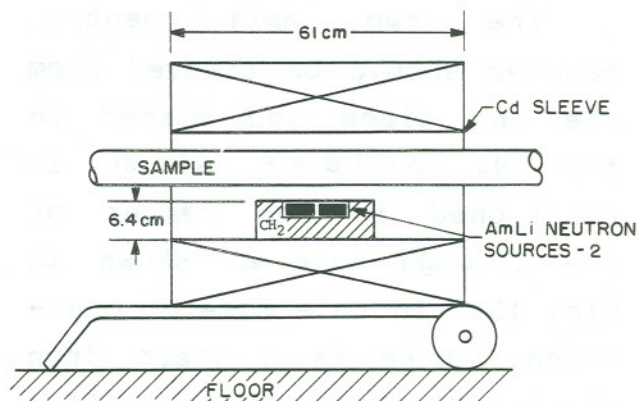


Fig. 13.  
Schematic diagram of AWCC showing side operation to accommodate long samples such as fuel rods and trays.

2. If sample container height permits, place the 5-cm thick Al spacer on the bottom of the assay well. This is possible for containers that are less than 15-cm tall. By positioning the bottom of the sample at 5 cm, the next 10 cm of the counting well are in the flat response region (see Section IV-B). This geometry should be satisfactory for most HEU buttons and small cans.

3. For larger sample containers, open the geometry of the sample cavity but make sure that the calibration took place with the same configuration.

4. Insert the magnetic card in the HP-97 that corresponds to the desired assay program and printout format. Details concerning the HP-97 software programs are given in Ref. 1.

5. Attempt to position each sample in the well in the same relative position and record available information on gross weights and fill heights.

#### D. Calibration

Calibration of the system should be performed with samples that match the assay samples as closely as possible. Important parameters are enrichment, uranium density, and size. Because the calibration curve is nonlinear, more than one calibration standard is normally needed. For those cases where the calibration standards are inadequate, computer calculation methods are being developed to help bridge the gap.

The calibration standards are used to generate the fitting parameters for the selected functional form. Examples of such functions are:

$$R = a(1 - e^{-bm}) ,$$

$$R = \frac{am}{1 + bm} , \text{ and}$$

$$R = am + bm^2 .$$

where R is the real coincidence response and m is the fissile mass. Other forms might be required to match the particular sample category. Once the desired functional form and parameters have been



established, day-to-day operation can usually be accomplished using a "normalization" sample to confirm that the system has not changed. If minor shifts have taken place, a simple renormalization is usually possible.

If it is necessary to calibrate the system at a location distant from the subsequent assay location, it is desirable to measure a normalization sample at the time of calibration and to measure the same sample at the assay location. If this is not possible because of lack of material or transportation problems, the AmLi sources in the end plugs can be used to check the system. If these sources give the same net totals rate at the time of calibration and assay, then that gives a reasonable confirmation that the electronics have not changed. However, the neutron interrogation efficiency is not checked by this procedure. It is desirable to have physical standards at the assay location when possible.

Once the calibration function and fitting parameters have been established, these can be put in the HP-97 via the magnetic program card. Detailed procedures for doing this will be developed elsewhere.

#### IV. PERFORMANCE CHARACTERISTICS

##### A. Introduction

The performance of the AWCC depends on the configuration of the end plugs and sample cavity. The data referred to in this section will correspond to the "normal" configuration as shown in Figs. 1 and 4 unless stated otherwise. The configurations with larger sample cavities will generally have slightly lower counting rates and larger statistical errors, but a more uniform spatial response.

The performance characteristics are summarized in Table III. The coincidence counting rates are not of high importance because the statistical error is dominated by the accidental coincidence rate. The real coincidence counting rate increases by a factor of  $\sim 70$  in going from fast-neutron interrogation to thermal-neutron interrogation. The sensitivity limit is  $1 \text{ g } ^{235}\text{U}$  for the thermal-neutron mode and  $23 \text{ g } ^{235}\text{U}$  for the fast-neutron mode.



TABLE III  
PERFORMANCE CHARACTERISTICS OF AWCC

	<u>Neutron Interrogation</u>	
	<u>Thermal Mode</u>	<u>Fast Mode</u>
Low Enrichment U <sub>3</sub> O <sub>8</sub>	11 counts/s g <sup>235</sup> U	0.15 counts/s g <sup>235</sup> U
High Enrichment Metal	NA	0.10 counts/s g <sup>235</sup> U
Sensitivity Limit <sup>a</sup>	1 g <sup>235</sup> U	23 g <sup>235</sup> U
Measurement Precision(1000 s)	1.5%/20 g <sup>235</sup> U	3.8%/200 g <sup>235</sup> U

---

<sup>a</sup> Defined as net coincidence signal equal to 3 of background for 1000 s count.

---

In this case sensitivity is defined as a net signal level equal to three times the standard deviation of the background for a 1000 s measurement time.

#### B. Sample Position Effects

For assay applications, it is desirable to have a uniform response for all locations within the measurement chamber. To help achieve this goal, AmLi sources are located in both the top and bottom end plugs. This symmetric source arrangement gives a more uniform vertical response. The uniformity is helped by the fact that the efficiency for counting the induced-fission neutrons is greatest in the central section of the well counter. to measure the spatial response uniformity, a flat disk sample (1-cm-thick) containing 500 g of <sup>235</sup>U was measured at increments from the bottom to the top of the chamber, with the AmLi source positioned in both the bottom and top plugs. The induced response vs height is given in Fig. 14. The response is uniform ( $\pm 2\%$ ) for sample fill heights between 5 and 18 cm. For a single source located in the bottom, the response changes by more than a factor of 4 over the same height range.

Table IV gives the relative response as a function of sample fill height for two cases. The first case corresponds to the recommended configuration with the 5-cm-tall spacer under the container to obtain better uniformity. The second case corresponds to a tall (>15 cm) container placed directly on the bottom of the assay chamber with no spacer. In the second case the response is about 6% larger for fill heights of 1-2 cm as compared with the middle region. However, for the case using the spacer, the fill height has a negligible (<1%) effect for fillings of 9 cm or less.

It is very likely that fill height considerations related

to geometry and material position will be secondary to self-shielding absorption and matrix material effects.

If we consider a small sample rather than a large container with different fill heights, then the response as a function of position is shown in Fig. 15. Again the response is very uniform if we avoid the 5 cm regions on the top and bottom. The radial response drops off by ~5% near the walls because then the sample is farther from both AmLi sources than when it is in the center.

For the configurations using a larger sample cavity (e.g., Fig. 5), the fractional response variation with position change is less than the above case. Figure 16 shows the vertical response for a configuration with a 30-cm tall sample cavity. In this case the response was uniform ( $\pm 2\%$ ) for fill heights between 4 and 24 cm.

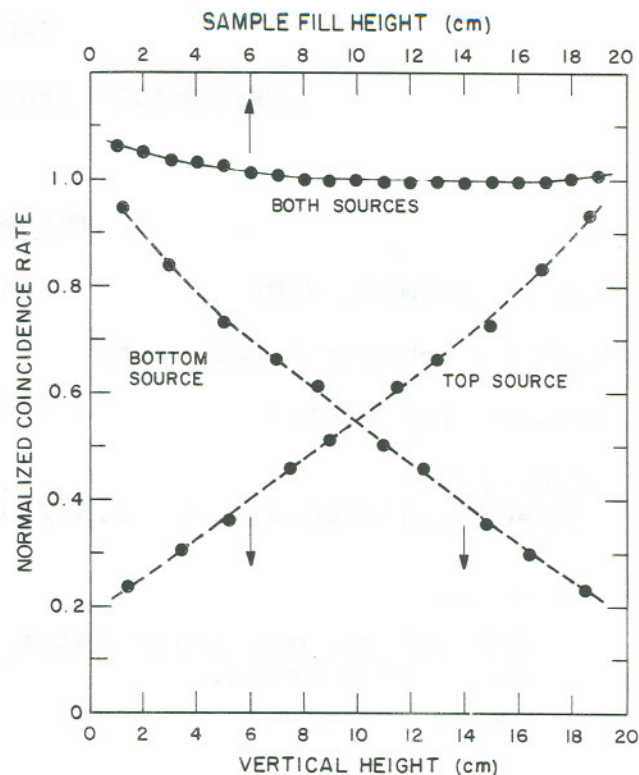


Fig. 14.

Coincidence response as sample fill height for the AWCC in normal configuration (see Fig. 4) using single source (bottom curves) and double source (top curve).



TABLE IV  
GEOMETRIC EFFECT OF SAMPLE FILL-HEIGHT  
ON COINCIDENCE RESPONSE FOR 20-cm HIGH CAVITY

<u>Sample Fill Height (cm)</u>	<u>Can on 5-cm Spacer</u>	<u>Relative Response 10-cm Can on Bottom</u>
1	0.996	1.060
2	0.997	1.050
3	0.998	1.040
4	0.999	1.031
5	1.000	1.021
6	1.002	1.015
7	1.004	1.011
8	1.007	1.005
9	1.010	1.001
10	1.014	1.000
11	1.019	0.998
12	1.025	0.996
13	-	0.995
14	-	0.995
15	-	0.998
16	-	1.000
17	-	1.001
18	-	1.005
19	-	1.010

In summary, very good spatial uniformity has been achieved without any movement of the sample or sources. As long as the sample is placed on top of the spacer and in the center of the cavity, no corrections are necessary in the data analysis.

#### C. Neutron Interrogation Penetrability

For most applications involving high enrichment uranium, it is desirable to have good penetration into the sample with the interrogation neutrons. This reduces the number of standards needed for the calibration and makes the assay less subject to error because of a mismatch between the sample and the standards. For these reasons, fast-neutron interrogation is normally used with the AWCC. However, the walls and end plugs of the AWCC are made of  $\text{CH}_2$  and this introduces a significant number of low-energy neutrons that are above the Cd cut-off energy. These neutrons are primarily responsible for the nonlinear, self-shielding characteristic of the calibration curve.

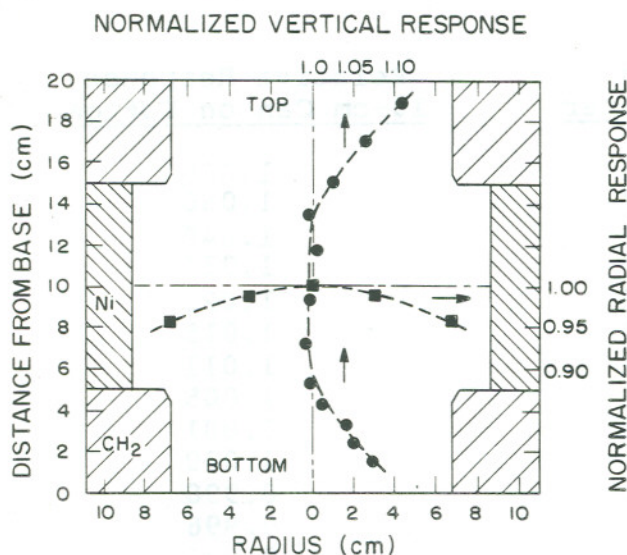


Fig. 15.

Vertical and radial coincidence response vs sample position for a small disc sample. The AWCC is in its normal configuration as shown in Fig. 4.

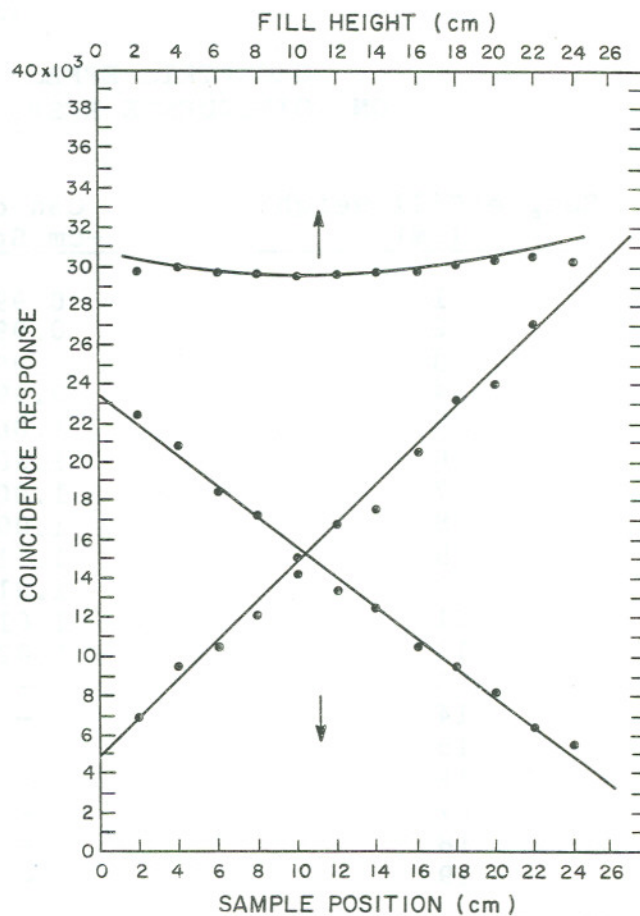


Fig. 16.

Coincidence response vs sample fill height for the AWCC using single source (bottom curves) and double source (top curve). In this case the cavity is opened to a 30 cm vertical height.

To help improve the neutron penetration and response linearity, a 2.54-cm-thick Ni reflector is placed on the wall of the sample cavity. The nickel liner improves the counting statistical error as well as the response linearity as a function of sample mass. This liner, which acts as a fast-neutron reflector for the AmLi interrogation neutrons, reduces the statistical error by ~25%. To evaluate the usefulness of the nickel in improving response linearity, we counted uranium (93% enriched) metal disks (6-cm diameter) in the center of the AWCC. The disks were stacked on top of each other to obtain the higher mass values; thus the



self-shielding of the neutrons increased as the stack thickness increased. The neutron source was placed in both the top and bottom plugs to make negligible the geometric effect of the stack height. Figure 17 shows the coincidence response for the cases with and without the nickel liner. The response for the nickel case is more linear but the problem is not severe for either case.

The increase in the response at the higher mass values ( $>2,000\text{g U}$ ) is caused by sample multiplication of the induced fission neutrons. For

this type HEU metal button, the self-shielding effect of the interrogation neutrons causes a drop in the calibration curve as the mass increases; whereas, the multiplication effect causes an increase in the curve with increasing mass. For the important mass range between  $\sim 800\text{--}3000\text{g U}$  these two effects nearly cancel each other resulting in a linear calibration curve, i.e., a uniform response per g U. This fortuitous result is somewhat subject to sample geometry, but geometric configurations which reduce multiplication, also reduce the self-shielding of the interrogation neutrons. For the low mass region ( $<1000\text{g U}$ ) the self-shielding effect dominates, and for the high mass region ( $>3000\text{g U}$ ), the multiplication effect dominates.

To check this effect of sample size, a series of 7-cm-diam. buttons were counted after completing the measurements with the 6-cm-diam. buttons. These larger diameter buttons had a response that was 2.2% higher on the average than the 6-cm buttons.

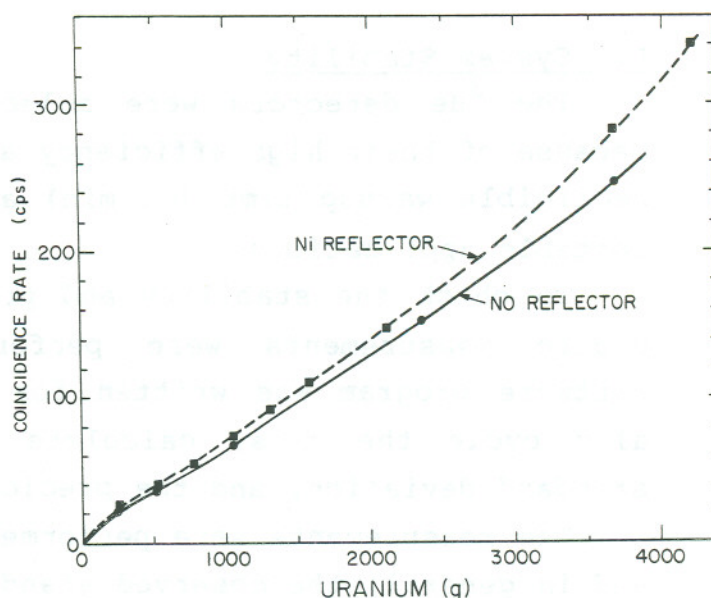


Fig. 17.  
Coincidence response vs uranium mass for HEU metal buttons in the AWCC with (top curve) and without (bottom curve) the Ni liner.

#### D. System Stability

The  $^3\text{He}$  detectors were selected for the present application because of their high efficiency and good stability. They require negligible warmup time ( $\sim 1$  min) and have proven to be durable for portable applications.

To check the stability and precision of the AWCC, a series of cyclic measurements were performed using a  $\text{U}_3\text{O}_8$  sample. A software program was written for the HP-97 that would automatically cycle the runs, calculate the running mean, the observed standard deviation, and the predicted standard deviation.

The measurements were performed over several three day periods, and in general, the observed standard deviations compared well with the calculated values. For example, for a three day period ( $\sim 30$  cycles) the measured  $\sigma$  was 0.9% and the calculated value was 0.8% for the net coincidence counts. For the total counts, the measured  $\sigma$  was 0.05% and the predicted value was 0.02%. For precisions of less than 0.1%, we would expect the measured  $\sigma$  to be greater than the calculated  $\sigma$  because of systematic errors dominating at this low level.

In summary, the AWCC system has operated with good stability. Software programs have been written for the HP-97 to automatically cycle the system and calculate the standard deviation. This should be useful for field applications, because the performance of the system can be automatically checked overnight.

#### ACKNOWLEDGEMENTS

The design of the detector was performed by S. Beach, L. Speir, and G. Walton, and T. Dye designed and fabricated the cart and electronic support. Helpful discussions on the design of the system were held with J. Foley, N. Ensslin, M. Krick, R. Walton, and C. Hatcher. Evita Medina Ortega helped with the measurements and data evaluation.



## APPENDIX A

### CALCULATION OF PERFORMANCE CHARACTERISTICS

The totals (singles) counting rate is given by

$$T \approx \epsilon_{\alpha} S + \text{sample contribution},$$

where  $S$  is the AmLi ( $\alpha, n$ ) source intensity and  $\epsilon_{\alpha}$  is the efficiency for counting the AmLi source. For most uranium assay applications, the sample contributes a negligible fraction of the total neutrons and the sample term can be neglected. The accidental coincidence rate  $A$  is given by

$$A = GT^2 \approx G(S\epsilon_{\alpha})^2,$$

where  $G$  is the coincidence gate length. It can be shown that the minimum error is achieved when the gate length  $G$  is set equal to 1.2 times the neutron lifetime  $\tau$  of the detector. To first-order approximation, the real coincidence rate  $R$  is given by

$$R \approx KU S \epsilon_f^2,$$

where  $U$  is the mass of  $^{235}\text{U}$ ,  $\epsilon_f$  is the efficiency for counting the induced fission neutrons, and  $K$  is a constant that includes the fraction of real events in the coincidence gate length  $G$  or  $1.2\tau$ , the fission cross section, the number of neutrons emitted per fission, and the geometric coupling between the interrogation source and the sample. the net signal-to- background ratio is given by

$$\frac{R}{A} = \frac{KU}{1.2\tau} \cdot \frac{1}{S} \cdot \left( \frac{\epsilon_f}{\epsilon_{\alpha}} \right)^2.$$

The smaller interrogation sources,  $S$ , will give higher signal-to-background ratios. Also any improvement in the  $\epsilon_f/\epsilon_{\alpha}$  ratio will be squared in its effect on the signal-to-background ratio.

The relative statistical error in the measurement is given approximately by

$$E \approx \frac{\sqrt{R + 2A}}{R} \approx \frac{\sqrt{KUS\epsilon_f^2 + 2.4\tau S^2\epsilon_\alpha^2}}{KUS\epsilon_f^2} \quad (1)$$

For large interrogation source intensities ( $S \geq 10^5$ ), the R term under the radical is negligible and the relative error simplifies to

$$E = \frac{\sqrt{2.4\tau}}{KU} \cdot \frac{\epsilon_\alpha}{\epsilon_f^2},$$

and it becomes apparent that significant error reductions can be made by increasing the efficiency for counting the induced fission,  $\epsilon_f$ . For instance, if by selective  $\text{CH}_2$  shielding and neutron moderation,  $\epsilon_\alpha$  is reduced by a factor of 2 and  $\epsilon_f$  increased by a factor of 2, the relative error would be reduced by a factor of 8. Stated differently, the assay time to obtain a given precision would be reduced by a factor of 64.

To evaluate the influence of the source strength S on the relative error, we calculated Eq. (1) for different values of S. The constants K,  $\epsilon_f$  and  $\epsilon_\alpha$  were determined from measurements with the high-level neutron coincidence counter (HLNCC).<sup>1</sup> Figure 18 shows the relative error vs S for the HLNCC and the estimated values for the AWCC. Source strengths as low as  $\sim 10^4$  n/s can be used with little loss in assay precision and the error is independent of S for values of S greater than  $10^5$  n/s. A 1000-s measurement for a 200-g  $^{235}\text{U}$  sample results in a relative error of  $\sim 15\%$  for the HLNCC and  $\sim 3\%$  for the AWCC when both units have the same cavity height.

In practice, the larger source strengths ( $> 10^5$  n/s) do not perform as well because of their larger physical size ( $\sim 5$ -cm-diam. x 13-cm-long). The 5-cm diameter displaces  $\text{CH}_2$  in the end plug shields thereby increasing  $\epsilon_\alpha$ , and the long length effectively increased the distance between the sample and the source S.



For small sources ( $< 2 \times 10^4$  n/s) the background neutrons from the room and the source might contribute a significant fraction of the counts in the accidental coincidence rate A. The present AWCC uses two sources with yields of  $4.7 \times 10^4$  n/s each giving a combined source strength S of  $9.4 \times 10^4$  n/s.

For applications involving high neutron background levels such as plutonium samples, then it is desirable to use a larger source strength (e.g.,  $\sim 10^6$  n/s) to override the neutron rate from the sample.

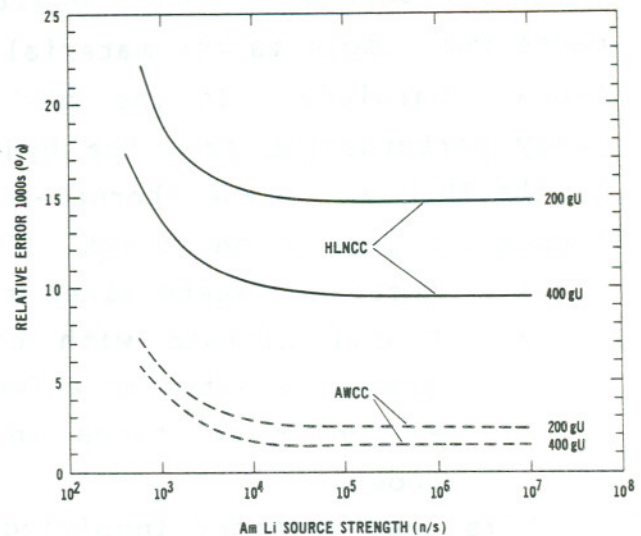


Fig. 18.  
Calculated relative precision as a function of neutron interrogation source strength for the HLNCC and the AWCC with 20-cm-high sample cavities.

## APPENDIX B

### THERMAL-MODE OPERATION

The AWCC can be used for measurement applications involving small amounts of fissile material ( $< 50$  g  $^{235}\text{U}$ ) by converting to the thermal-neutron interrogation mode. To avoid severe self-shielding problems, the  $^{235}\text{U}$  should have a low concentration and not be in the form of lumps. This is always the case for low enrichment uranium because of the uniformly large fraction of  $^{238}\text{U}$ . Examples of this type material are  $\text{U}_3\text{O}_8$  powder and  $\text{UO}_2$  pellets. Examples of high enrichment uranium with a low concentration of fissile material are  $^{235}\text{U}$ -Th and  $^{233}\text{U}$ -Th mixtures found in high temperature reactor (HTR) fuels. In this case the fissile concentration is low because the uranium is mixed with much larger quantities of thorium and graphite. Also, some types of scrap and waste would fit into this general category.

Materials that normally contain large quantities of hydrogenous materials should be measured with the AWCC in the thermal-mode because the sample matrix material thermalizes the interrogation neutrons regardless. If the AWCC is in the fast-neutron mode, the assay perturbation from the hydrogenous matrix is large; however, if the AWCC is in the thermal-mode, the additional hydrogen in the sample has less of an effect. Examples of this type material are:

1. Scrap and waste mixed with rubber gloves or plastic bags.
2. Uranyl nitrate with concentrations ranging from a few grams per liter to a few hundred grams per liter.
3. Plutonium solutions in the same concentration range as above.

This last category involving Pu solutions would require both a passive (i.e., removal of the AmLi sources) coincidence count to obtain the  $^{240}\text{Pu}$  effective, and an active interrogation to obtain the fissile content. Clearly more research and development is needed before the AWCC can be applied to this category of material.

To set up the AWCC for thermal-mode operation, do the following:

1. Remove the Ni liner from the well using the thumb screws provided with the unit.
2. Lift out the Cd sleeve which lines the sample well.
3. Remove the Cd cap and Cd disc on the lid and bottom plug.
4. Replace the 5-cm tall  $\text{CH}_2$  rings on both the lid and bottom plug.

It is not necessary to remove the bottom plug from the well to remove the Cd. A screwdriver is required for the above steps and the entire operation should take less than 10 min.

To evaluate the AWCC in the thermal-mode, measurements were made on a set of cans containing low enriched  $\text{U}_3\text{O}_8$ . The cans, shown in Fig. 12, had a diameter of 10.5 cm and a height of 12.5 cm. The cans typically contained 1 kg of  $\text{U}_3\text{O}_8$  with the  $^{235}\text{U}$  enrichment ranging from 0.7-10%.

The results of the measurements are shown in Fig. 19. The net coincidence response is nonlinear as a function of  $^{235}\text{U}$  content because of neutron self-shielding in the  $\text{U}_3\text{O}_8$ . The sample



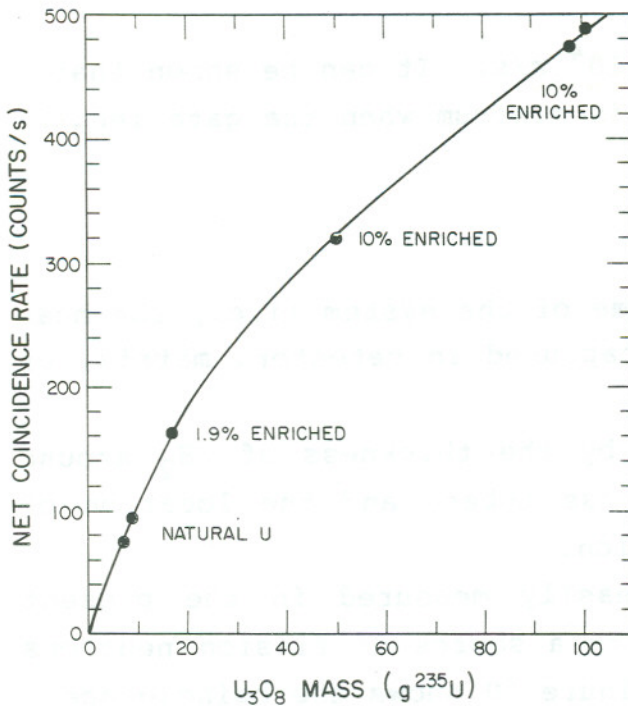


Fig. 19.  
Coincidence rate vs  $^{235}U$  mass  
for low enrichment  $U_3O_8$   
samples and thermal-neutron  
interrogation mode.

containing 16.8 g  $^{235}U$  gave a 2.2% standard deviation for a 1000-s count.

## APPENDIX C

### ERROR CALCULATION AND GATE LENGTH SELECTION

The statistical error in the measurement is dominated by the accidental coincidence rate  $A$  and this rate is directly proportional to the gate length  $G$ ,

$$A = T^2 G$$

for a uniform totals rate  $T$ . Thus, it is desirable to keep  $G$  as small as possible and still include most of the time correlated coincidence neutrons.

The standard deviation in the measurement can be approximated by

$$\sigma = \sqrt{(R+A) + A}$$

$$\sigma \approx \sqrt{2A} ,$$

for AmLi source strengths of  $>2 \times 10^4$  n/s. It can be shown that the fractional standard deviation is minimum when the gate length

$$G \approx 1.2\tau ,$$

where  $\tau$  is the neutron die-away time of the system (i.e., the mean time for a fission neutron to be captured in detector, matrix, or to leak from the system).

The value of  $\tau$  is controlled by the thickness of  $\text{CH}_2$  around the detectors, the number of  $^3\text{He}$  gas tubes, and the location of the Cd sleeves for neutron absorption.

The die-away time  $\tau$  can be easily measured in the present unit by varying the gate length with a source of fission neutrons (e.g., U or  $^{252}\text{Cf}$ ) in the well. Figure 20 shows the coincidence rate for gate settings ranging from 8-128  $\mu\text{s}$  and with a fixed pre-delay of 4-5 s for the HLNCC and AWCC systems. These curves have the functional form

$$R = (1 - e^{-G\tau}) ,$$

where they are normalized to unity for very large gate values. Fitting the AWCC data shown in Fig. 20 gives a value of  $\tau \approx 50 \mu\text{s}$  and thus the optimum gate setting is 64  $\mu\text{s}$ . For the HLNCC,  $\tau \approx 30 \mu\text{s}$  because it has less  $\text{CH}_2$  in the body.

To check the effect of gate setting on the assay error, we have calculated the fractional standard deviation from the data for the different gate settings. Figure 21 shows the relative error which has been normalized to unity at a 64  $\mu\text{s}$  gate setting. We see that the error increases by 20% for a 32  $\mu\text{s}$  gate and 18% for a 128  $\mu\text{s}$  gate. Thus, the AWCC unit is normally operated with a gate setting of 64  $\mu\text{s}$  and it is not necessary to change this value for routine operation. The AWCC should always be operated with the same gate setting used during the calibration.



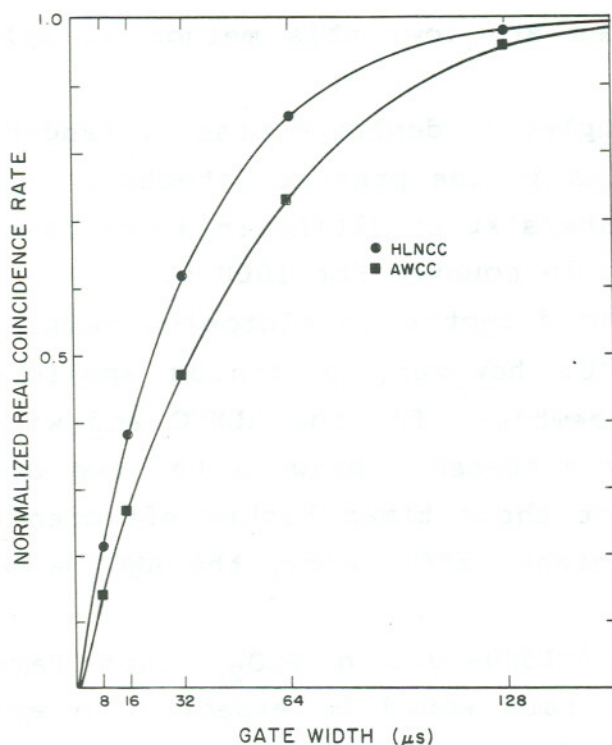


Fig. 20.  
Normalized coincidence rate vs gate width for the HLNCC and the AWCC.

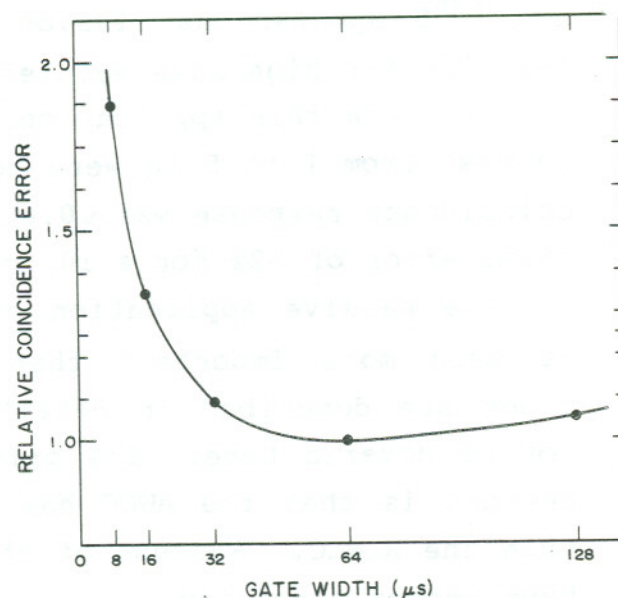


Fig. 21.  
Relative assay error vs gate width with the error normalized to unity at its minimum value ( $\sim 64 \mu$ s).

#### APPENDIX D

##### PASSIVE-MODE OPERATION

The AWCC can be operated in the passive neutron coincidence mode to measure  $^{238}\text{U}$  or  $^{240}\text{Pu}$ . For kilogram quantities of low enrichment  $\text{UO}_2$ , the passive neutrons from the spontaneous fission of  $^{238}\text{U}$  can be counted with the coincidence circuitry. The half-life for this reaction is  $\sim 9.86 \times 10^{15}$  years resulting in a spontaneous fission neutron yield of  $1.1 \times 10^{-2}$  n/s.g. Thus, a 10 kg sample of  $\text{UO}_2$  (low enrichment) gives a fission neutron yield of  $\sim 110$  n/s. If the inspector is confident of the enrichment, he can measure the  $^{238}\text{U}$  in the passive coincidence mode and deduce the  $^{235}\text{U}$  content. If, however, the enrichment is not known, the  $^{238}\text{U}$  can be measured in the passive mode and the  $^{235}\text{U}$  can be measured in the passive mode and the  $^{235}\text{U}$  in

the active mode to directly determine the enrichment. Because the  $^{238}\text{U}$  spontaneous fission rates are low, this method is only feasible for high mass samples.

To check this application, samples of depleted uranium ranging in mass from 1 to 5 kg were counted in the present detector. The coincidence response was  $\sim 0.6$  counts/s\*kg resulting in a statistical error of  $\sim 2\%$  for a 10 kg sample counted for 1000 s.

The passive application of the detector to plutonium samples is much more important than  $^{238}\text{U}$ ; however, plutonium applications are described in detail elsewhere<sup>1</sup> for the HLNCC and will not be covered here. The primary difference between the two detectors is that the AWCC has about three times higher efficiency than the HLNCC. Because of this higher efficiency, the AWCC will have better precision.

For high mass  $\text{PuO}_2$  samples ( $>1500$ - $2000$  g  $\text{PuO}_2$ ) that have a high  $^{240}\text{Pu}$  content, the totals rate would be expected to exceed 150-200 kHz. This would overload the electronic circuitry and it would be necessary to reduce the efficiency and also, hopefully, the die-away time. One method of doing this is to put a thin Cd or boron sleeve around some or all of the  $^3\text{He}$  tubes. Additional development work is needed before the AWCC can be applied to plutonium samples with such high counting rates.

To convert the detector to the passive mode, the AmLi sources are removed from both end plugs. The neutron sources should be placed far enough from the detector so as not to greatly increase the room background rate.

#### REFERENCES

1. Merlyn Stewart Krick and Howard O. Menlove, "The High-Level Neutron Coincidence Counter (HLNCC): Users' Manual", Los Alamos Scientific Laboratory report LA-7779-M (1978).
2. H. O. Menlove, N. Ensslin, C. R. Hatcher, E. Medina, and J. Foley, "Active Well COincidence Counter," Los Alamos Scientific Laboratory report LA-7211-PR (1977) pp. 7-10.



3. J. E. Foley and M. M. Thorpe, "Random Source Interrogation: A New Nondestructive Assay Technique," Los Alamos Scientific Laboratory report LA-4705-MS (1971) pp. 9-12.
4. Nuclear Safeguards Research Program Status Report, Sept.-Dec. 1975, Los Alamos Scientific Laboratory report LA-6316-PR (April 1976) pp. 1-4.
5. J. E. Swansen, N. Ensslin, M. S. Krick, and H. O. Menlove, "A New Shift Register for High Count Rate Coincidence Applications," Los Alamos Scientific Laboratory report LA-6788-PR (1977) pp. 4-6.
6. T. W. Crane, "Gas Mixture Evaluation for  $^3\text{He}$  Neutron Detectors," Los Alamos Scientific Laboratory report LA-7030-PR 1978) pp. 39-40.
7. M. M. Stephens, J. E. Swansen, and L. V. East, "Shift Register Neutron Coincidence Module," Los Alamos Scientific Laboratory report LA-6121-MS (1975).

